J Electroceram (2012) 28:246–255
DOI 10.1007/s10832-012-9722-7

Dielectric properties and scaling behavior of lithium tungsten phosphate glasses

M. H. Shaaban

Received: 18 August 2011 / Accepted: 23 March 2012 / Published online: 12 April 2012

Abstract In the present study a series of ternary (30 Li_2O, (70-x) P_2O_5, xWO3) glasses were prepared and their dielectric properties and ac conductivity were investigated. The measurements have been taken in the frequency range from 100 Hz to 100 kHz and over the temperature range from 296 K to 578 K. The temperature dependence of ac conductivity can be adequately explained by considering the contributions from mixed ionic and electronic mechanisms. In the studied glasses it is found that the ac conductivity increases with increasing frequency. By investigating the relation between temperature and the frequency exponent "s" of the power law $\sigma_{ac}=A\omega^s$, it is found that the Correlated Barrier Hopping model (CBH) is appropriate for describing the conduction mechanism in the samples. In an attempt to investigate the universality of ac conductivity in these glasses, it is found that the data obtained follow Rolling scaling model. When considering the dielectric properties, it is found that the M″vs. M′ plots give master Cole-Cole curves at all temperatures. These results can be considered as an indication of the presence of space charge or accumulation of charges in some regions inside the samples. The relation between M″/ $M_{max''}$ and f/f_p represent a master plot at different temperatures. These scaling suggest the existence of a distribution of potential wells, in which the carriers are trapped.

Keywords Lithium tungsten phosphate glasses · Dielectric properties · ac conductivity and scaling models

M. H. Shaaban (✉)
Chemistry Department, Faculty of Science, Tanta University, Tanta, Egypt
e-mail: mhani55@hotmail.com

1 Introduction

Oxide glasses have many advantages, e.g. composition diversity, good chemical durability and easy mass production at low cost [1]. Among the various oxide glasses, phosphate glasses have several advantages over silicate and borate glasses, e.g. low glass transition temperature (T_g), optimizing coefficient of thermal expansion and high UV transmission. Owing to these features, many studies have been conducted on the various properties and structure of phosphate glasses [2–4]. Oxide glasses containing transition metal ions (TMI) are of great interest, because of their technological applications. In particular, the transition metal ions (such as tungsten, vanadium, molybdenum, iron, and copper) can have the role of either glass formers and /or glass modifiers in multi-component glasses [5], which provide a wide range of properties and new applications by selecting and tailoring chemical composition . Tungsten oxide containing glasses have unusual electro-chromic and photosensitive properties, which are attributed to the ability of tungsten atoms to exist in glass in various oxidation states (W^{+6}, W^{+5} or W^{+4}). The tungsten oxide units participate in the glass network [6] creating considerable improvement of the chemical durability and thermal stability against devitrification [7].

It is well known that the conductivity of the alkali metal containing glasses, which do not contain transition metal oxides, is due to mobility of the alkali cations [8]. When glass contains transition metal oxides, instead of alkali cations, the conductivity is known to be electronic. The mechanism which is responsible for the electronic conduction is a thermally activated hopping of electrons from low to high valence states [9]. When a glass contains alkali cations and transition metal ions, a mixed electronic and ionic conduction is expected. The

conductivity of such glasses as a function of alkali content frequently exhibits a minimum similar to the mixed alkali ions effect [10]. Recently, the mixed ionic-electronic conductors glasses have an attracted interest due to their potential applications in electrochemical cells and electro-optical devices [11].

The structure and the electrical properties of alkali phosphate glasses that contain WO_3 or MoO_3 have been frequently studied. Studer et al. [12] reported that in K_2O–WO_3–P_2O_5 glasses the ratio W^{+6} /W^{+5} decreases as K_2O is introduced. Bazan et al [13] noticed that the addition of Li_2O to (xLi_2O–$55WO_3$–$(45\text{-}x)P_2O_5$) glasses produces the sharpest drop in the electrical conductivity, when the WO_3 content is held constant. On the other hand, addition of Li_2O to (xLi_2O–$(60\text{-}x)$ WO_3–$40P_2O_5$) leads to more gentle diminution in conductivity up to 20 mol% Li_2O, where the WO_3 content reaches its lowest values. They argued that the mobile electrons (or polarons formed by the capture of electron by a W^{+6} atom) are attracted to oppositely charged Li^+ ions, which form neutral cation-polaron pairs. This effect designated as the "ion-polaron-effect" or IPE. Boudlish et al [10] reported an increase in W^{+5} concentration with the addition of Li_2WO_4 to Li_2O–Li_2WO_4–P_2O_5 glasses, where the WO_3 content is kept constant. They related such increase to the loss of oxygen during glass preparation and its subsequent stabilization in glass. They also noticed that the larger the Li_2WO_4 content, the larger will be the electronic conductivity of the glass. . Bih et al [14] reported that in $0.25Li_2$ O–$0.75[x(MoO_3)2$ –$(1\text{-}x)(P_2$ $O_5)]$ glasses, Mo^{+5} /Mo_{tot} and Mo^{+5} /Mo^{+6} ratios evaluated from the analysis of EPR spectra have shown the existence of maxima for $x \approx 0.27$. They deduced that such glasses are mainly electronic conductors. The electrical conductivity increases with increasing x for $0.27 \leq x \leq 0.45$, whereas and reaches constant value for $x \approx 0.45$. The ionic electrical conductivity decreases rapidly when x increases for the lower x values (≥ 0.27). The electronic conductivity may be assumed to be due to electronic hopping from the lower valence state, Mo^{+5} (donor level), to the higher valence state, Mo^{+6} (acceptor level), where the interaction between the electrons and lattice is sufficiently strong to produce a small polaron [15]. To the best of our knowledge, there are no reports on the effect of substitution of P_2O_5 by WO_3 on the electrical properties of Li_2O–P_2O_5- WO_3 glasses. In addition, it was highly interesting to study the dynamics of relaxation mechanism of alkali tungsten phosphate glasses.

The objective of the present work is to study the effect of replacement of P_2O_5 by WO_3 on the dielectric properties of lithium phosphate glasses. The frequency, temperature and WO_3 concentration dependence of the ac conductivity have been analyzed, in an attempt to investigate the conduction and relaxation mechanism in these glasses. We have discussed the possibility of scaling the frequency dependent values of conductivity at different temperatures into one single "master" curve. The electrical modulus formalism has been extensively discussed for studying electrical relaxation behavior.

2 Experimental

2.1 Glass preparation

Reagent grade $(NH_4)H_2PO_4$, WO_3 and Li_2CO_3 were used as starting materials for preparing the phosphate glass compositions. For each composition, a total of 30 g of raw materials were weighed and mixed in a mortar. Each mixture was melted in an alumina crucible at 1200°C for 0.5 h in air, and was poured into a cold graphite mold. The samples were then annealed at 573°C for 3 h to remove any stresses that are generated in glass during cooling. The X-ray diffraction technique was used to confirm the glassy nature of the prepared composition.

2.2 ac and dc conductivity measurements

The samples were prepared in the form of discs of 10 mm diameter, and polished by usual techniques to a thickness of 2 mm. Each sample was coated with colloidal silver paste on both sides. The samples were annealed at 100°C for 2 h to ensure the good adherence between the electrode and the sample surfaces. The constructed cell for the electrical measurements consists of a silica tube surrounded by nickel chrome wire as a heater. A (chromel-alumel) thermocouple (inside the tube) was used for temperature measurements. The ac conductivity was measured by applying a complex impedance technique. A constant ac voltage ($V_{r.m.s}$=1 V) was applied to the sample . The current passes through the sample was determined by measuring the potential difference across an ohmic resistor connected in series to the sample by using a lock- in amplifier (Stanford Research System SR510). The lock-in amplifier simultaneously measures the voltage across the resistor and the phase difference ϕ between this voltage and the applied voltage on the sample. Since the voltage drop on the ohmic resistance is in phase with the current I, therefore it can be assumed that ϕ is the phase angle between the voltages drops on the sample and the current I passing through it. The ac conductivity σ_{ac}, the dielectric constant $\varepsilon^{\backslash}$, the imaginary part of permittivity $\varepsilon^{\backslash cr}$, the real and imaginary parts of the electric modulus M* and the dielectric loss $\tan\delta = \frac{1}{\tan\phi}$, were calculated using a computer program. To overcome the effect of humidity the electrical conductivity was measured under vacuum. The measurements were made at temperatures from room temperature 296 K up to 578 K. Furthermore

the dc conductivity was measured by applying a constant voltage (10 V) and measuring the current, then application of Ohm's Law. The current was measured using Keithley Electrometer type 617

3 Results and discussion

3.1 ac and dc conductivities

Figure 1(a) represents the temperature dependence of the dc conductivity in the temperature range of (296–578 K) for the glassy system (30 Li_2O, (70-x) P_2O_5 , xWO_3) where x= 0,5,10,15, 20 and 25 mol%. The temperature dependence of the dc conductivities can be represented by a set of straight lines. The linear relationship between the logarithm of dc conductivity and inverse of temperature for all the samples indicates that the following Arrhenius relation is satisfied:

$$\sigma_{dc} = B \exp(-\Delta E_{dc}/kT) \quad (1)$$

where B is a constant for a given glass, k is Boltzmann's constant and ΔE_{dc} is the activation energy for the dc conduction. The values of ΔE_{dc} and σ_{dc} at room temperature are included in Table 1. It is clear that the dc conductivity decreases and ΔE_{dc} increase with increasing WO_3 concentration up to 10 mol% WO_3, where the dc conductivity has the lowest values of conductivity. Beyond 10 mol% WO_3, an increase in the dc conductivity and a decrease in ΔE_{dc} were observed. The conductivity of alkali metal containing glasses is ionic [8]. However in tungsten phosphate glasses the electronic conduction was attributed to hopping of electrons from the W^{+5} to W^{+6} ions [16]. Thus It can be assumed that with the addition of WO_3 up to 10 mol% a mixed ionic-electronic conduction mechanisms operation are simultaneously obtained, where formation of ion-polaron pair tend to decrease the conductivity and increase in the ΔE_{dc} values in agreement with observed by [13]. The increase in dc electrical conductivity and decrease in ΔE_{dc} with increasing WO_3 content beyond 10 mol% , could be attributed to that the electronic conduction becomes the predominant one ,where as the increase in W^{+5} concentration with increasing WO_3 content, increases the electronic conduction [10]. It has also been reported that in some glasses containing both alkali metal cations and transition metal ions, electrical transport is mainly electronic since alkali metal cations have small mobility.[13, 14, 16].

The relation between the ac conductivity and the WO_3 concentration are represented in Fig. 1(b). Such relation shows a similar behavior which was observed in the dc electrical conductivity. The frequency dependence of the ac conductivity at different temperatures for two of the studied glasses is presented in Fig. 2(a and b). At room temperature, the ac conductivity shows linear frequency dependence. However at higher temperatures, the ac conductivity exhibits less frequency dependent conductivity plateau at lower frequencies, whereas at higher frequencies a dispersion region is observed (increase of ac at higher temperatures with increasing frequencies). Similar behavior has been also observed for all the other compositions. This plateau is attributed to the long-range translational motion of ions contributing to dc conductivity dc [16]. At lower frequency the ac conductivity is approximately equal to the measured σ_{dc} conductivity. Figure 2(a and b) reveals that the switch over of the frequency independent region to frequency dependent region at higher frequencies, shifts to higher

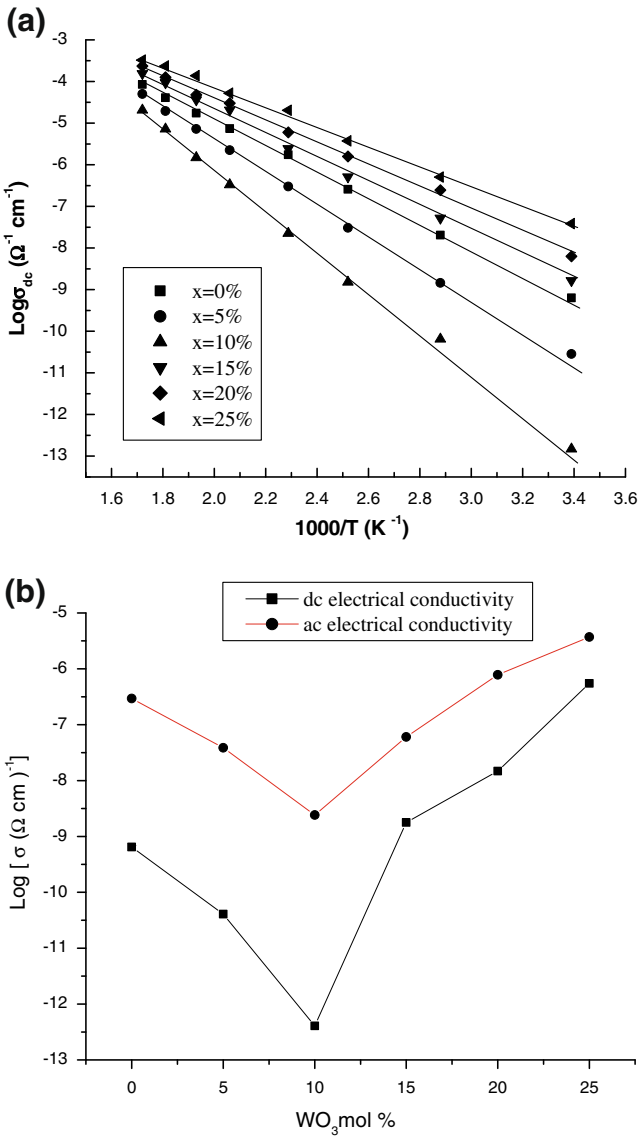

Fig. 1 (**a**) The relation between the Log σ_{dc} and 1/T measured as a function of WO_3 content (x=WO_3 mol%). (**b**) The relation between the WO_3 content (mol%) and both the dc and the ac electrical conductivities

Table 1 (σ_{dc}) the dc electrical conductivity, (ΔE_{dc}) the actvation energy of the dc conductivity ,(s) the power law exponent, (β) value (equation 8) and (N) the concentration of localized states of (30 Li_2O, (70-x) P_2O5, xWO_3) glasses

Sample	WO_3mol%	σ_{dc} (Ω^{-1} cm^{-1})	ΔE_{dc} (eV)	s	β	W_m (eV)	N
1	0	6.76×10^{-10}	0.785	0.94	0.06	0.988	7.4×10^{13}
2	5	2.88×10^{-11}	0.807	0.855	0.145	1.062	8.07×10^{13}
3	10	1.474×10^{-13}	0.853	0.8752	0.1248	1.239	4.615×10^{13}
4	15	1.81×10^{-9}	0.818	0.83	0.17	0.905	8.9×10^{13}
5	20	6.32×10^{-9}	0.695	0.822	0.178	0.865	1.5×10^{14}
6	25	7.244×10^{-8}	0.445	0.76	0.24	0.641	4.5×10^{14}

frequencies with increasing temperature. This behavior implies the onset of conductivity relaxation. The observed dependence of dispersion on the conductivity is due to the fact that the inhomogenities in the glasses may be of a microscopic nature with the distribution of relaxation processes through distribution of energy barriers [17]. The frequency

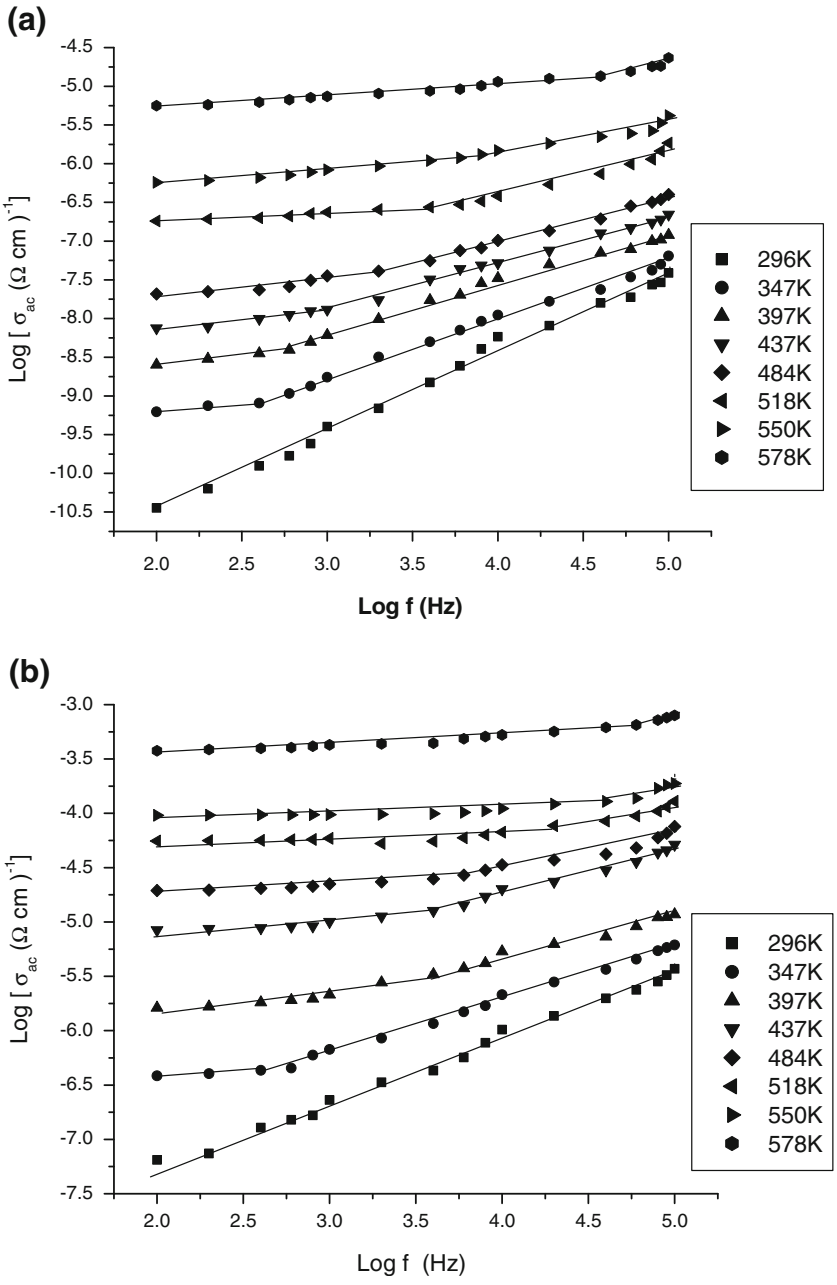

Fig. 2 (**a**) The relation between the Log σ_{ac} and Log frequency at different temperatures for sample 2. (**b**) The relation between the Log σ_{ac} and Log frequency at different temperatures for sample 6

dependence region at higher frequency satisfies the universal power law empirical relation [18]:

$$\sigma(\omega) = \sigma(o) + A\omega^{s} \tag{2}$$

where σ(o) is the dc conductivity,

$$\sigma_{ac} = A\omega^{s}, \tag{3}$$

A is a constant and s is the power law exponent. The values of the exponent s displayed as a function of temperature in Fig. 3. The s values are almost less than unity and decrease with temperature. The numerical values of s at room temperature are in the range 0.64<s<0.94. Hill and Jonscher [19] observed such behavior for the ac conductivity in a wide range of materials, including a number in which conduction by hopping is expected. They reported that the exponent s typically covered the range 0.5–1 at room temperature. They also noticed that in most cases the values of s show a tendency to increase to unity as the temperature decreases. Elliot [20] proposed the correlated barrier-hopping model (CBH) and applied it to glassy semiconductors. According to this model, barrier hopping of bipolarons (i.e. two electrons hopping between charged defects D+ and D−) has been proposed to interpret the frequency dependence of conductivity in glass. Thus electrons in the charged defect state hop over the columbic barrier whose height is given as W according to Eq. (4):

$$W = W_m - \frac{4ne^2}{\varepsilon R} \tag{4}$$

Where W_m is the maximum height of the energy band, ε is an effective dielectric constant; e is electronic charge, n the number of electrons that hop (n=2) [21] and R is the distance between the hopping sites. The relaxation time τ for the electrons to hop over a barrier of height W is given by Eq. (5):

$$\tau = \tau_o \exp(-W/kT) \tag{5}$$

where τ_o is the order of an atomic vibration period . τ_o value is assumed to be ($\approx 10^{-13}$ s) for oxide glass system [21] and k is Boltzmann constant. The final expression for the ac conductivity can be expressed by Eq. (6):

$$\sigma ac = \left[\frac{\pi^2 N^2}{24}\varepsilon' \left(\frac{8e^2}{\varepsilon' W_M}\right)\frac{s}{\tau_o^{\beta}}\right] \tag{6}$$

where N is the concentration of localized states and β is given by Eq. (7):

$$\beta = \frac{6kT}{W_m} \tag{7}$$

$$\text{and } s = 1 - \beta \tag{8}$$

Using eqs. (6)–(8) the density of state N can be calculated. The N, and s and W values for the studied glasses, at room temperature and at frequency equal to 1 KHz are listed in Table 1 . In the CBH model the exponent s is predicted to be frequency and temperature dependent, with s values increasing towards unity as temperature decreased. The data obtained from Table 1 and Fig. 3 clearly represented that the CBH model seems to be appropriate theory for the AC conductivity in the studied glasses.

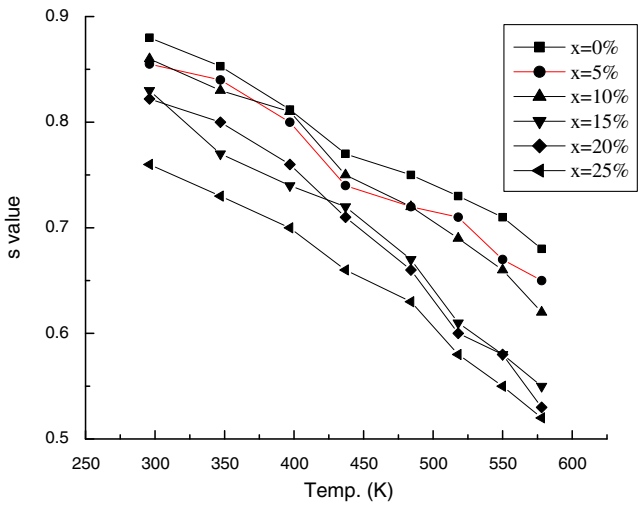

Fig. 3 Variation of the frequency exponent s value with temperature for different glass compositions (x=WO_3 mol%).

3.2 Scaling model of ac conductivity

Many trials of scaling data had been done to investigate the universality of ac conductivity properties in disordered solids . Although some methods of scaling were complicated [22, 23] ,others were simple [24–26]. Scaling is defined as a method of treating data, this method allows one to subsume a mass of frequency response data by means of a master curve whose shape is independent of any independent variable, such as temperature or mobile ion concentration [30]. In other words, scaling is a process of making a set of curves, representing the frequency dependence of some functions at different temperatures or concentrations and then to collapse such curves into one single master curve representing the phenomenon in a general sense. The dc conductivity is a parameter that is frequently used in scaling methods. Therefore we have performed a scaling process of the ac conductivity as a function of frequency in Fig. 4(a, b), which show the conductivity master curves of the samples 3 and 6, where we used Log (σ_{ac} /σ_{dc}) as the y-axis scaling parameter and Log (f / Tσ_{dc}) as the x-axis scaling parameter.

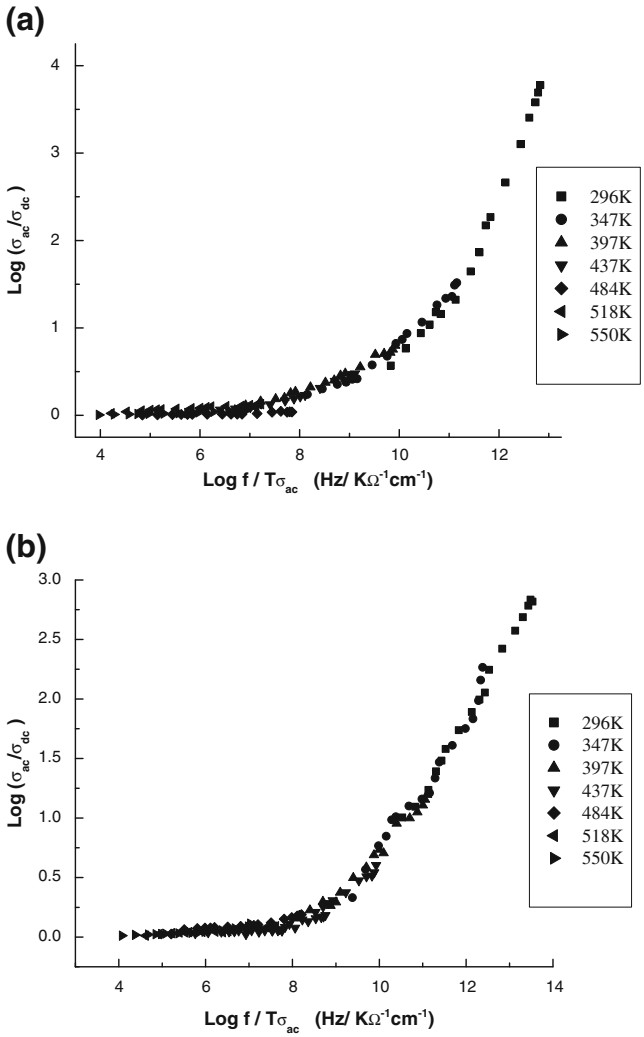

Fig. 4 (**a**) The relation between Log(σ_{ac}/σ_{dc}) and Log (f / Tσ_{dc}) at different temperatures for sample 2. (**b**) The relation between Log(σ_{ac}/σ_{dc}) and Log (f / Tσ_{dc}) at different temperatures for sample 6.

This scaling is known as Roling scaling [26], who found that the product Tσ_{dc} obeys an Arrhenius relation, and he also obtained conductivity master curves for some ionic conducting glasses by using this scaling parameter. From the Fig. 4(a, b) it is obviously seen that the conductivity increases with increasing the frequency. The collapse of ac conductivity values at different temperatures in a single master curve reveals our success in constructing the master curves for the samples, which indicate that the relaxation in conductivity may be considered as a temperature independent process. In other words, we can say that the quite satisfying overlap of the data at different temperatures on a single master curve illustrates well that the dynamic processes occurring at different frequencies need almost the same thermal activation energy. Another indication of those scaled master curves is that all "Arrhenius" temperature dependence of conductivity is embedded in the dc conductivity term [27].

3.2.1 The dielectric constant $\varepsilon^{\backslash}$ and the dielectric loss tan δ

The values of $\varepsilon^{\backslash}$ show considerable temperature dependence, exhibiting larger values at lower frequencies as noticed from Fig. 5(a). Prasad et, al [28] studied the dielectric properties of PbO borate glass containing MoO_3 . They reported that the considerable increase of dielectric constant values with temperature can be attributed to the space charge polarization associated with bonding defects [29]. Figure 5(a) illustrates that, the dielectric constant has higher values at lower frequencies and at higher temperatures which are normal in oxide glasses. Thus at lower frequencies, the charge carriers hop easily out of the sites with low free energy barriers in the electric field direction and tend to accumulate at sites with high free energy barriers. This leads to a net polarization of the ionic medium and gives higher dielectric constant values. However at high frequencies, the charge carriers will no longer be able to rotate sufficiently rapid, so their oscillation

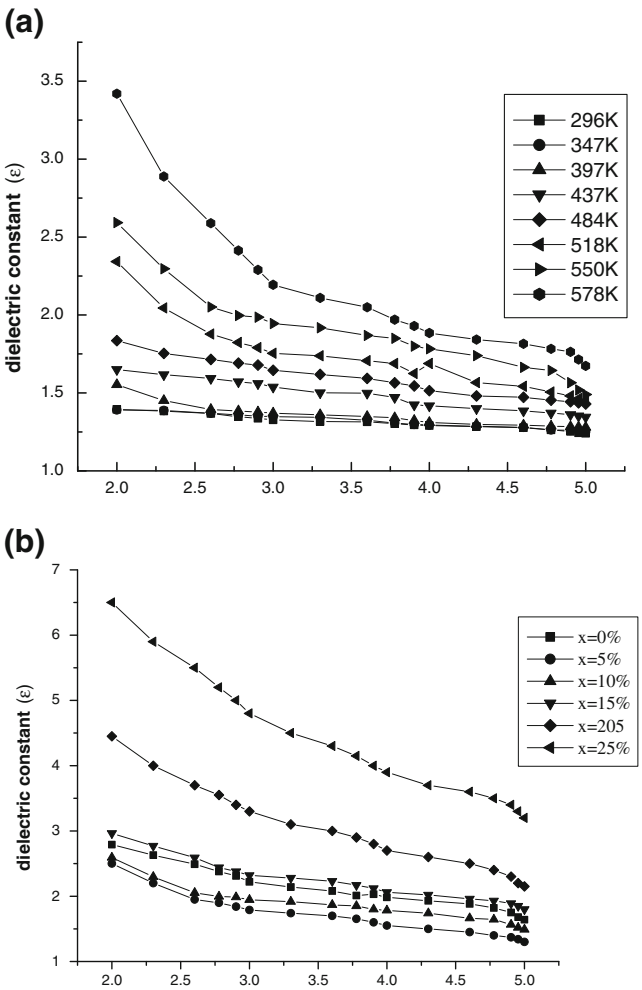

Fig. 5 (**a**) The relation between Log dielectric constant (ε) and Log frequency for sample 3 (x=10%mol%). (**b**) The relation between log frequency and the dielectric constant (ε) for different glass samples (x=WO_3 mol%)

will begin to lay behind this field resulting in lower dielectric constant values [30]. Figure 5(b) represents an increase in the dielectric constant ($\varepsilon^{\backslash}$) values with the increase of WO_3 content of the glass. This behavior explained as WO_3 content increase, a gradual conversion of W^{+5} to W^{+6} ions in the glass network takes place[16] . W^{+6} ions act as modifiers, weaken the glass network and ,thus create pathways suitable for migration of free ions that build up space charge. Thus, the weaker the network the much more is the space charge polarization which leads to an increase in the dielectric constants values [10, 28]. This conclusion is further supported by the results that with increasing WO_3 content in alkali phosphate glasses, the degree of deformation of glass network will increase bonding defects, which in turn increase the space charge polarization causing an increase in the values of dielectric parameters [7, 31].

The frequency dependence of tan δ of glass containing 20 mol% WO_3 at different temperatures is shown in Fig. 6. The curves exhibit distinct maxima (ω_{max}). Such maximum shifts towards higher frequency with increasing temperature. It is known that maxima in the loss tangent versus frequency curves occur when the conductance is proportional to the square of the applied frequency . This explains the shift towards higher values with increasing temperature (i.e. energy is supplied to charge carriers) [32]. The relaxation time tan can be obtained from the equation:

$$\mathrm{Tan}\ \delta\,\omega_{\max} = 1 \tag{9}$$

The relation between τ and temperature obeys the following equation:

$$\tan\delta = \tau_o \exp(-\Delta E_{\tan\delta}/\mathrm{k\,T}) \tag{10}$$

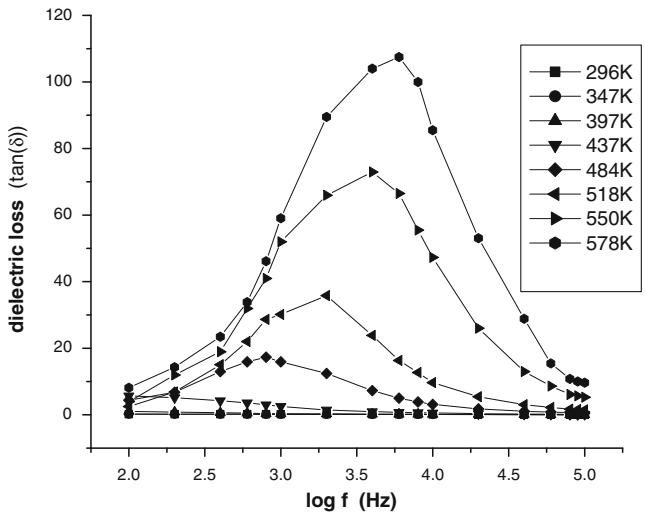

Fig. 6 The relation between the dielectric loss (tanδ) and Log frequency for sample 5

where τ_o is constant , k is Boltzmann constant and $\Delta E_{\tan\delta}$ is the activation energy of relaxation. The values of activation energy of relaxation are approximately equal to the activation energy of dc conductivity ΔE_{dc} , as presented in table [2] . It is noticed that sample 1did not show ω_{max} , which may be explained on the basis that the sample is having a maximum at lower frequency than the measured range.

3.3 The electrical modulus formalism

The electrical modulus formalism has been extensively used for studying electrical relaxation behavior in ion conducting materials [33]. The advantage of this representation is that the electrode polarization effects are minimized in this formalism. In the modulus formalism, an electric modulus M* is defined in terms of the reciprocal of the complex relative permittivity ε*.

$$M* = 1/\varepsilon* = M' + \mathrm{j}\,M'' \tag{11}$$

where M′ and M″ are the real and imaginary parts of the complex modulus M*

Saafan et al. [34] investigated the Cole-Cole diagrams of both M″ vs. M′ at different temperatures; they found that these diagrams are suitable way for representation of the experimental data. They concluded that the Cole-Cole diagrams, the one giving a master semicircular curve for all temperatures and it will also be an indication to the property that is dominating in the studied glass. The use of M*(ω) has the meaning of the following relationship[35]:

$$E = M * D \tag{12}$$

Which is the reverse of the more commonly used relationship

$$D = \varepsilon * E \tag{13}$$

where E is the electric field vector, D is the electric displacement vector, M* is the complex function of the electric modulus and ε* is the complex function of the permittivity. The physical significance of these two representations is that in equation (13) the electric field E is the independent variable, which determines the dielectric displacement, while the reverse is true of equation (12) where D is the independent variable. Now, it happens frequently that the great majority of practical situations involve the electric field as the independent variable, and accordingly equation (13) is applicable. There are only relatively few situations where the opposite is the case in [34]. One such example is the motion of space charge ρ_v in a dielectric system where the resulting D field is directly related through:

$$\mathrm{Div}\,D = \rho_v \tag{14}$$

It is then desired to calculate the resulting electric field one would have to use equation (12) [35]. Some

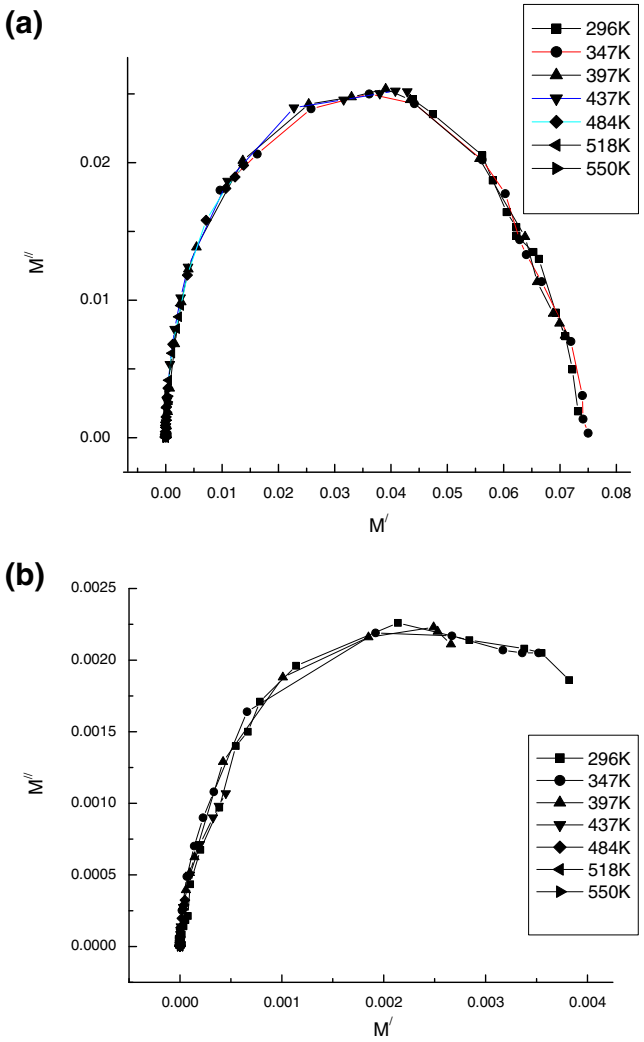

Fig. 7 (**a**) The relation between $M^{//}$ and $M^{/}$ at different temperatures for sample 3. (**b**) The relation between $M^{//}$ and $M^{/}$ at different temperatures for sample 6

Table 2 (ΔE_{relax}) the activation energy of relaxation, ($\tau_{tan\delta}$) the relaxation time of the dielectric loss and ($\tau_{M''}$) the normalized relaxation time of (30 Li_2O, (70-x) P_2O5, xWO_3) glasses

Sample	ΔE_{relax} (eV)	$\tau_{M''}$ at 211°C	$\tau_{tan\delta}$ at 211°C
2	0.871	2.71×10^{-8}	5.85×10^{-8}
3	0.827	2.86×10^{-8}	6.01×10^{-8}
4	0.713	3.19×10^{-8}	6.64×10^{-8}
5	0.477	3.47×10^{-8}	7.46×10^{-8}

researchers stated that one should be careful when using M* representation in some cases of comparative analysis of the ion transport properties of different solids , since it may result in misleading interpretations of the ion dynamics [27, 36]. Figure 7(a, b) show that the glass under investigation belong to the category of materials which satisfy equation (12), i.e. we can say that there must be a considerable space charge in these glasses. The presence of such space charge has been mentioned before in section 3.3, to interpret the dielectric constant measurements concluded by Prasad [28], and is in agreement with his findings.

The variation of normalized-imaginary parts M''/M''_{max} of complex electric modulus with frequency, at various temperatures show a slightly asymmetric peak at each temperature, as can be seen in Fig. 8. The frequency range below the peak-frequency f_p determines the range in which charge carriers are mobile on long distances. At frequency above M''_{max}, the carriers are spatially confined to potential wells, being mobile on short distances making only localized motion within the wells. The maximum of modulus spectra M_{max}'' shifts towards the higher frequencies, with increase of temperature Fig. 1. This behavior suggests that the spectral intensity of the dielectric relaxation is activated thermally in which hopping process of charge carriers are

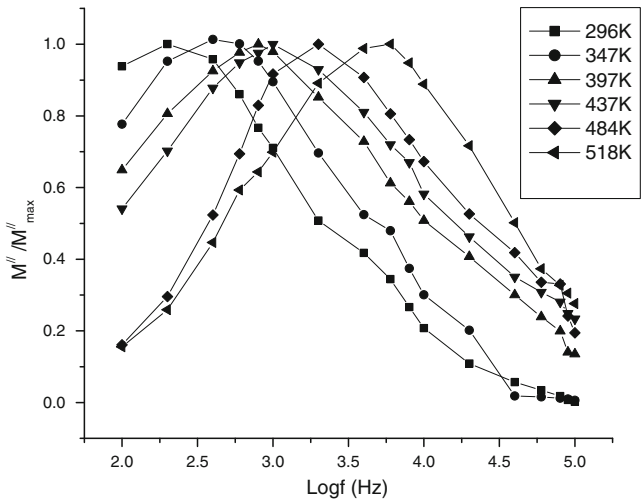

Fig. 8 The relation between $M^{//}/M_{(max)}{}^{//}$ and Log f (Hz) f0r sample 3

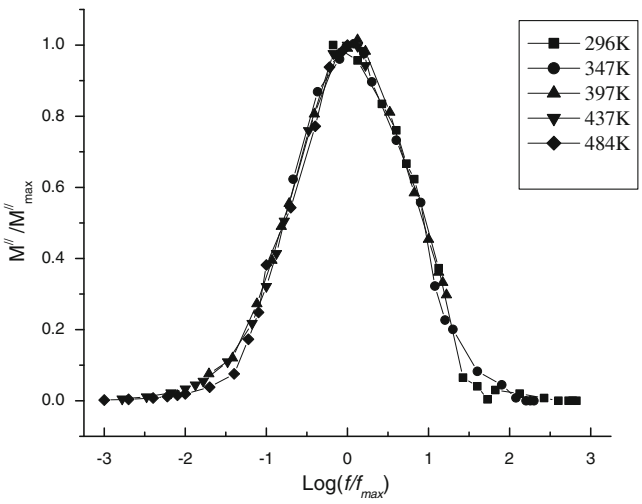

Fig. 9 The relation between $M^{//}/M_{(max)}{}^{//}$ and Log (f /f $_{(max)}$) for sample 3

taking place [37]. Also, shifting of the peak frequencies in the forward direction with temperature implies that the relaxation time decreases with increasing of temperature. The peak frequency, f_p, corresponding to the maximum in M''/M''_{max} as a function of frequency, Fig. 8, is found to be typically correlated with the average conductivity relaxation time $\tau_{M''}$. From the condition $\omega_c\tau_{M''}=1$, thus ($\tau_{M''}=1/2\pi f_p$) [38]. The $\tau_{M''}$ and the $\tau_{tan\delta}$ values of the various compositions are given in Table 2

It is observed that the relaxation time corresponding to dielectric loss $\tau_{tan\delta}$ is smaller than that corresponding to the normalized parameters ($\tau_{M''}$). Gerhardt [39] concluded that the bulk response in terms of localized condition, i.e., defect relaxation or non-localized conduction, i.e., ionic/electronic conductivity is determined by comparing the dielectric loss and dielectric modulus. The non-localized process such as dc conductivity is dominating at low frequencies. Thus, the high dielectric loss is usually accompanied by rising $\varepsilon'(\omega)$ at low frequencies. Such type of behavior is noticed in the present study. In the present study, the observed values of high dielectric constant at low frequency (Figs. 5a,b) could explain the smaller values of $\varepsilon'(\omega)$ and smaller relaxation times for the localized relaxation processes when compared to the non-localized relaxation processes [40].

Figure 9 represent a master plot of the modulus isotherms, where the y-axis is scaled by M″max and x-axis is scaled by the peak frequency *f*p. The curves show a high degree of superimposing at different temperatures. This behavior indicates that the dynamical processes are temperature independent, which was observed. The scaling of the frequency by fp parameter gives a distribution of M''/M''_{max} values considering logarithmic representation at around log $f/f_{max}=1$. At frequency range above this value, some degree of dispersion can be observed depending on the glass formulation and temperature of measurement. Considering previous assumptions, it is possible to hypothesize the existence of a distribution of potential wells, in which the carriers are trapped [41–43].

4 Conclusion

For the prepared lithium tungsten phosphate glasses [30 Li, (70-x) PO_4 , xWO_3] (x=0,5,10,15,20and 25%),the activation energy values decrease and the ac conductivity values increase with increasing WO_3 content of the glass up to10mol% WO_3 . This behavior has been considered as an indication to the presence of a mixed electronic and ionic conduction mechanisms. The increase in dc electrical conductivity and decrease in ΔE_{dc} with increasing WO_3 content beyond 10 mol% , could be attributed to that the electronic conduction becomes the predominant one. The variation of ac conductivity with frequency follow the power law $\sigma_{ac}=A\omega^s$. The decrease in the exponent s with decreasing temperatures suggested that the correlated barrier hopping model (CBH) is appropriate for describing the conduction mechanism.

By investigating the ac conductivity in these glasses, the data obtained follow Rolling scaling. The master curves for the ac conductivity indicate that the relaxation in conductivity may be considered as a temperature independent process, where all the temperature dependence has been proved to be embedded in the scaling parameters. The dielectric constant values increase with increasing the WO_3 content of the glass, suggesting that the WO_3 ions seem to occupy the interstitial positions of the glass, contributing to the polarization. The considerable increase of dielectric constant values with temperature can be attributed to the space charge polarization. The relation between M″ vs. M′ gives a master semicircular curve for all temperatures. This is another indication to the presence of space charge i.e. accumulation of charges in some regions inside the samples. This finding reinforces the interpretation considered for the dielectric constant. The variation of normalized-imaginary parts M″/ Mmax″ with the frequency scaled by the peak frequency fp represent a master plot at different temperatures. These scaling are suggesting the existence of a distribution of potential wells in which the carriers are trapped.

Acknowledgment The authors wish to thank Prof. M.K.El-Nimer , physics Department, Faculty of Science, Tanta University for allowing us to carry out the experimental work ac measurements electrical conductivity and for fruitful discussions.

References

1. R.H. Doremus, Glass Science, 2nd edn. (Johh Wiley 1973)
2. K.U. Kumar, P. Babu, K.H. Jang, H.J. Seo, C.K. Jayasankar, A.S. Joshi, J. Alloy. Comp. **458**, 509 (2008)
3. N. Hashima, Y. Mayumiand, J. Nishii, Mater. Sci. Eng. B **161**(1–3), 91 (2009)
4. M. Elisa, B. Sava, A. Diaconu, D. Ursu, R. Patrascu, J. Non-Cryst. Solids **355**, 1877 (2009)
5. G.D. Khattak, A. Mekki, M.A. Gondal, Appl. Surf. Sci. **256**(11), 3630 (2010)
6. M. von Dirke, S. Mullar, M. Rager, J. Non-Cryst. Sol. **124**, 265 (1990)
7. P. Subbalakshmi, N. Veeraiah, Phys. Chem. Glass **42**, 307 (2001)
8. M.D. Ingram, Phys. Chem. Glasses **28**, 215 (1987)
9. H. Hirashima, K. Nishi, T. Yoshida, J. Am. Ceram. Soc. **66**, 7070 (1983)
10. D. Boudlish, L. Bih, M. Archidi, M. Haddad, A. Yacoubi, A. Nadiri, B. Elouadi, J. Am. Soc. **85**, 623 (2002)
11. L. Bih, L. Abbas, A. Nadiri, H. Khemakhem, B. Elouadi, J. Mol. Struct. **872**, 1 (2008)
12. F. Studer, N. Rih, B. Raveau, J. Non-Cryst. Solids **107**, 101 (1988)
13. J.C. Bazan, J.A. Duffy, M.D. Ingram, M.R. Mallace, Solid State Ionics **86–88**, 497 (1996)
14. L. Bih, L. Abbas, S. Mohdachi, A. Nadiri, J. Mol. Struct. **891**, 173 (2008)

15. M.H. Hekmat-Shoar, C.A. Hogarth, G.R. Moridi, J. Mater. Sci. **20**, 889 (1985)
16. L. Murawski, R.J. Barczynski, Solid State Ionics **176**, 2145 (2005)
17. R. Murugaraj, G. Govindaraj, and Deepa George. Mater. Lett. **57**, 1656–1661 (2003)
18. A.K. Jonscher, Nature **267**, 673 (1977)
19. R. Hill, A. Jonscher, J. Non-Cryst. Solids **32**, 53 (1979)
20. S. Elliot, Adv. Phys. **36**, 135 (1987)
21. M.K. Elkholy, R.A. El-Mallawany, Mater. Chem. Phys. **40**, 163 (1995)
22. P.K. Dixon, L. Wu, S.R. Nagel, Phys. Rev. Lett. **65**(9), 1108 (1990)
23. N. Menon, S.R. Nagel, Phys. Rev. Lett. **74**(7), 1230 (1995)
24. D.L. Sidebottom, J. Zhang, Phys. Rev. B **62**(9), 5503 (2000)
25. B. Roling, A. Happe, K. Funke, M.D. Ingram, Phys. Rev. Lett. **78** (11), 2160 (1997)
26. J.R. Macdonald, J. Appl. Phys. **90**(1), 153 (2001)
27. S.A. Saafan, Phys B Condens Matter **403**, 2049 (2008)
28. P. Syam Prasad, B.V. Raghavaiah, R. Balaji Rao, C. Laxmikanth, N. Veeraiah, Solid State Commun. **132**, 235 (2004)
29. M. Prashant Kumar, T. Sankarappa, S. Kumar, J. Alloys Compd. **464**, 393 (2008)
30. D.K. Durga, N. Veeraiah, Physica B **324**, 127 (2002)
31. P. Pergo, W.M. Pontuschka, J.M. Prison, Solid State Commun. **141**, 545 (2007)
32. A.K. Jonscher, *Dielectric relaxation in solids* (Chelsea Dielectric Press, London, 1983)
33. D.P. Almond, G.K. Duncan, A.R. West, Solid State Ionics **8**, 159 (1983)
34. S.A. Saafan, A.S. Seoud, R.E. El Shater, Phys. B **365**, 27 (2005)
35. A.K. Jonscher, *Universal relaxation law* (Chelsea Dielectric Press Ltd, London, 1996)
36. D.L. Sidebottom, B. Roling, K. Funke, Phys. Rev. B (2), 024301 (2000)
37. G.S. Nadkarni, J.G. Simmons, J. Appl. Phys. **41**, 545 (1970)
38. F.S. Howell, R.A. Bose, P.B. Macedo, C.T. Moynihan, J. Phys. Chem. **78**, 639 (1974)
39. R. Gerhardt, J. Phys. Chem. Solids **55**, 1491 (1994)
40. S. Duhan, S. Sanghi, A. Agarwal, A. Sheora, S. Rani, Physica B **404**, 1648 (2009)
41. A. Dutta, A. Ghosh, J. Non-Cryst. Solids **351**, 203 (2005)
42. S. Lanfredi*, P.S. Saia, R. Lebullenger, A.C. Hernandes, Solid State Ionics **146**, 329 (2002)
43. A.A. Ali, M.H. Shaaban, Solid State Sci. **12**, 2148 (2010)